World Journal of Biology Pharmacy and Health Sciences

eISSN: 2582-5542

Cross Ref DOI: 10.30574/wjbphs

Journal homepage: https://wjbphs.com/

(Review Article)

Check for updates

Next-Gen Magnetocaloric Cooling: MnFePSi Nanoparticles for Compact and Sustainable MCHP Systems

Shad Abdelmoumen Serroune [1,*], Ir. Khasani [2], Dr. Sandra Merrier [3], Stéphane Devilliers [4] and Tadeshi Ryushi [5]

[1] *Head and Chief Scientist, NanoGEIOS Laboratory – Nanotechnology and Advanced Materials, Miami, Florida, USA.*

[2] *Research Professor, Universitas Gadjah Mada (UGM), Yogyakarta, Special Region of Yogyakarta, Indonesia; Nanotechnology Consultant, Nanogeios Technologies, Miami, Florida, USA.*

[3] *Director of Development, Kaigen Nanoparticles, USA; Integration Specialist, Nanogeios, Miami, Florida, USA.*

[4] *Principal Scientist, Microscopy and Raman Spectroscopy, Nanogeios Laboratories, Miami, Florida, USA.*

[5] *Senior Researcher, Nanogeios Japan, Tokyo, Japan; Lead Engineer for Liquid NanoCO_2 Integration and Nanofusion Deployment with GEIOS Technologies, Miami, Florida, USA.*

World Journal of Biology Pharmacy and Health Sciences, 2024, 20(02), 1065-1092

Publication history: Received on 05 October 2024; revised on 22 November 2024; accepted on 25 November 2024

Article DOI: https://doi.org/10.30574/wjbphs.2024.20.2.0908

Abstract

This study introduces a groundbreaking magnetocaloric heat pump (MCHP) system that replaces traditional rare earth-dependent fixed-bed regenerators with a MnFePSi nanoparticle slurry (50 nm, 10% vol.), achieving simultaneous refrigerant and heat transfer functions. Experimental evaluations under controlled conditions (23°C ±0.2°C, 10 K span) demonstrate a 14.6% improvement in coefficient of performance (COP), 33.4% higher specific power density, and 24.8% system mass reduction compared to conventional gadolinium-based systems. The slurry's non-Newtonian rheology enables rapid thermal response (56.3% faster) and exceptional temperature uniformity (±0.8°C), while operating at frequencies up to 7.6 Hz.

Key innovations include a proprietary experimental platform integrating real-time spin-state monitoring, nano-Hall magnetic field mapping, and coupled CFD-ML modeling. Extended stability tests reveal minimal performance degradation (1.3% COP reduction over 48 hours) and negligible nanoparticle agglomeration (<2%). The complete elimination of rare earth elements reduces lifecycle environmental impact by **60%**, addressing critical sustainability challenges in cooling technology.

These results establish the first practical demonstration of a rare-earth-free magnetocaloric cooling system with superior efficiency, scalability, and material utilization—setting a new benchmark for sustainable thermal management solutions. The technology's compact design and enhanced heat transfer coefficients (22% improvement over fixed beds) position it as a transformative approach for next-generation refrigeration, air conditioning, and waste heat recovery applications.

Keywords: Magnetocaloric Effect (MCE); Nanoparticle Slurry; MnFePSi Alloy; Rare Earth-Free Cooling; Magnetocaloric Heat Pump (MCHP); Thermal Management

1. Introduction

This report presents quantitative experimental validation of a novel magnetocaloric heat pump (MCHP) system utilizing a patented nanoparticle-based magnetocaloric slurry as both the active refrigerant and heat transfer medium developed by NANOGEIOS Laboratories since April 2024.

* Corresponding author: Shad Abdelmoumen Serroune

Comprehensive testing under controlled laboratory conditions (23±1°C, 10K span, 200W cooling load) demonstrates statistically significant performance enhancements compared to conventional fixed-bed active magnetic regenerator (AMR) systems.

Key performance metrics were rigorously assessed through replicated trials (n=5), yielding the following results: coefficient of performance (COP) increased by 14.6% (4.62±0.08 vs. 4.03±0.11); specific power density improved by 33.4% (133.1±1.9 W/kg vs. 99.8±2.3 W/kg); system mass decreased by 24.8% (7.6 kg vs. 10.1 kg); and operating frequency increased by 49.0% (7.6±0.1 Hz vs. 5.1±0.2 Hz).

2. Test Setup and Methodology

The experimental evaluation of our nanoparticle-based magnetocaloric slurry system required the development of a specialized test apparatus capable of precise control and measurement of both magnetic and thermodynamic parameters. This section details the design considerations, instrumentation, and protocols employed to ensure rigorous comparison with conventional MCHP technology under identical operating conditions.

Our methodological approach focused on three critical aspects: (1) establishing controlled baseline performance metrics for a conventional fixed-bed MCHP system, (2) precise characterization of the magnetocaloric slurry's thermophysical and magnetic properties, and (3) comprehensive performance mapping of the integrated slurry-based system across relevant operating parameters. All testing was conducted in accordance with established protocols for magnetic refrigeration systems (ASTM E2197-20 and IEC 62552:2015), with appropriate modifications to accommodate the novel slurry-based configuration.

2.1. Experimental Apparatus

Our laboratory testing employed an advanced multi-physics experimental platform that synergistically combines physical measurements with Nanogeios' proprietary Virtual Digital Twin Environment and Molecular Data Center with H200 computational framework for real-time material characterization and system optimization. This hybrid approach enabled unprecedented insights into nanoparticle-fluid interactions and magnetocaloric phenomena at the nanoscale.

2.2. Flow Circuit Configuration

We constructed a precision-engineered flow circuit using specialized borosilicate tubing (10.0 mm ID) with embedded nanoscale surface modifications developed through our proprietary ion-implantation process. This surface treatment, unique to Nanogeios laboratories, minimizes boundary layer effects and enhances slurry-wall interactions. The circuit incorporated four critical zones:

- Magnetization Zone: Instrumented with our patented nano-Hall sensor array for 3D magnetic field mapping at 50μm resolution
- Hot-Side Heat Exchanger: Utilizing Nanogeios' thermo-conductive nano-composite plates with embedded quantum-dot thermal sensors
- Demagnetization Zone: Equipped with real-time magnetic relaxation monitoring
- Cold-Side Heat Exchanger: Incorporating phase-change monitoring with sub-millisecond temporal resolution

2.3. Magnetic Field Generation

Rather than relying on conventional magnetic assemblies, we utilized an advanced permanent magnet system designed and optimized through our proprietary H200 Virtual Digital Twin Environment and Molecular Data Center computational framework. The physical magnet assembly was engineered based on extensive simulations that explored optimal field configurations before manufacturing. This approach features:

Precisely engineered field gradients developed through simulation using our adaptive field reinforcement algorithm within the H200 computational environment, allowing us to test thousands of configurations virtually before physical implementation

Design optimization informed by computational models that simulate slurry magnetization states, enabling us to create physical magnet arrangements precisely matched to our fluid dynamics

High-precision physical field mapping with our nano-magnetometer array (±0.5 mT accuracy) providing real-world validation of our computational models

The H200 computational framework enabled us to virtually test multiple magnetic field configurations without requiring multiple physical prototypes, significantly accelerating our optimization process. Once the optimal configuration was identified through simulation, we fabricated the corresponding physical magnet assembly, resulting in superior field utilization compared to conventionally designed systems.

2.4. Advanced Material Characterization

Throughout testing, we employed Nanogeios' advanced material characterization suite to monitor nanoparticle behavior in real time. Our setup incorporated in-situ dynamic light scattering for continuous particle size distribution monitoring, enabling us to track any potential agglomeration processes as they occurred. We supplemented this with microfluidic sampling coupled with automated magnetic susceptibility analysis, allowing for precise measurement of the magnetocaloric properties during operation. The system also leveraged time-resolved X-ray absorption spectroscopy for tracking atomic-scale lattice dynamics during magnetization cycles, providing unprecedented insights into the structural changes occurring at the nanoscale. Perhaps most critically, our proprietary spin-state monitoring system delivered direct measurement of magnetic moment evolution, capturing the fundamental physics driving the magnetocaloric effect. These measurements fed directly into our computational models, creating a continuous feedback loop between experimental observations and theoretical predictions, thereby enhancing our understanding of the system dynamics and enabling real-time optimization.

2.5. Data Integration Framework

The experimental apparatus was fully integrated with our proprietary data fusion system that combines:

- Multi-modal sensor inputs from over 200 measurement points
- Real-time computational fluid dynamics simulations calibrated to actual flow conditions
- Atomistic modeling of nanoparticle magnetocaloric responses
- Machine learning algorithms for anomaly detection and system optimization

This integrated approach allowed us to observe phenomena impossible to capture with conventional instrumentation alone, particularly the nanoscale heat transfer mechanisms that drive the exceptional performance of our magnetocaloric slurry system.

By leveraging Nanogeios' unique capabilities in both advanced instrumentation and computational modeling, we were able to conduct experiments that transcend traditional laboratory testing, revealing fundamental material behaviors and system-level interactions that would remain hidden using conventional approaches.

2.6. Test Conditions

Our experimental evaluation was conducted under rigorously controlled conditions to ensure reproducibility, precision, and meaningful comparison between the novel nanoparticle-based magnetocaloric slurry system and conventional MCHP technology. We established a comprehensive testing environment leveraging Nanogeios' advanced climate control infrastructure and measurement capabilities.

2.7. Environmental Parameters

The testing environment was maintained using our ISO Class 6 (Fed. Std. 209E Class 1000) clean room facility equipped with:

- Precision HVAC system maintaining ambient temperature at 23 ± 0.2°C with spatial variation <0.3°C across the test platform
- Relative humidity control at 45 ± 2% to eliminate moisture-induced effects on thermal measurements
- Barometric pressure monitoring (101.3 ± 0.2 kPa) with automated data correction for pressure-dependent thermodynamic calculations
- Vibration isolation platform (eigenfrequency <2 Hz) to eliminate mechanical noise and ensure stable flow conditions
- Electromagnetic shielding (>60 dB attenuation) to prevent external fields from influencing magnetocaloric measurements

2.8. Thermal Loading Configuration

We established well-defined thermal boundary conditions using our proprietary microprocessor-controlled thermal load simulator. The system maintained a fixed temperature span (ΔT) of 10.00 ± 0.05K across the system using precision PID control, ensuring stable and reproducible testing conditions. Hot-side temperature was regulated at 28.00 ± 0.05°C using our six-stage cascade temperature controller, which provided exceptional stability even under varying load conditions. Complementing this, the cold-side temperature was maintained at 18.00 ± 0.05°C with active feedback compensation that continuously adjusted for any thermal drift. We generated a precise thermal load of 200.0 ± 0.5W using our calibrated resistive heater array with uniform heat flux distribution, eliminating hotspots that could skew performance measurements. The configuration also incorporated thermal mass simulators with programmable thermal capacitance to evaluate system response under dynamic conditions, allowing us to characterize performance under realistic load profiles rather than steady-state conditions alone. This comprehensive thermal management approach ensured that all performance comparisons between the conventional and nanoparticle-based systems reflected intrinsic technological differences rather than testing artifacts.

2.9. Slurry Preparation and Characterization

The magnetocaloric slurry was prepared according to our proprietary process and characterized using a comprehensive suite of analytical techniques. We began with a precisely metered volume of 1.000 ± 0.001 liters, ensuring exact concentration control critical for reproducible performance. Nanoparticle concentration was verified via multiple independent methods: magnetic susceptibility measurements, thermal diffusivity analysis, and direct mass fraction determination, providing cross-validation that enhanced measurement confidence. Rheological characterization was performed immediately before testing using our advanced rheometer with magnetic field capability to verify yield stress, viscosity, and thixotropic behavior under actual operating conditions, capturing the complex flow behavior relevant to system performance. We confirmed particle size distribution using dynamic light scattering to verify the absence of agglomeration that could compromise system efficiency. Additionally, zeta potential measurements were conducted to confirm suspension stability prior to testing, providing a quantitative metric of the electrostatic repulsion forces maintaining particle dispersion. This multi-parameter characterization approach ensured that the slurry properties remained consistent throughout testing and accurately represented the intended formulation.

2.10. Reference System Specification

For direct performance comparison, we utilized a meticulously calibrated conventional MCHP system:

- Active Magnetic Regenerator (AMR) bed containing 620g of high-purity gadolinium (99.9%, spherical particles, 250-425 μm diameter size fraction)
- Hydraulic diameter and porosity matched to provide equivalent pressure drop characteristics
- Identical magnetic field profile (1.03T maximum) applied using our standard permanent magnet array system
- Real-time data processing and simulation supported by our H200 Virtual Digital Twin Environment
- Matched heat exchanger geometry and thermal interface conditions
- Identical instrumentation and data acquisition protocols to eliminate measurement bias

3. Test Matrix Design

To ensure comprehensive evaluation, we implemented a full factorial test matrix exploring multiple operating parameters and their interactions. We systematically varied flow rates from 0.5 to 2.0 L/min in precise 0.25 L/min increments, capturing the full range of hydraulic conditions relevant to practical applications.

Operating frequencies were tested from 1 to 10 Hz in logarithmic steps, allowing us to characterize system performance across both conventional and high-frequency domains inaccessible to traditional systems. The thermal operating envelope was thoroughly mapped by testing cold-side temperatures from 5°C to 25°C and hot-side temperatures from 25°C to 45°C, encompassing conditions relevant to refrigeration, air conditioning, and heat pump applications.

We further expanded the test matrix by evaluating applied magnetic field strengths from 0.5T to 1.5T, quantifying system response to varying magnetocaloric driving forces. Each test condition was maintained until rigorous steady-state criteria were met, specifically temperature variations less than 0.05°C over a 10-minute period, ensuring that transient effects did not contaminate performance measurements.

Measurements were recorded for a minimum of 30 complete cycles at each operating point to ensure statistical validity and capture any cycle-to-cycle variations. This comprehensive testing approach, leveraging Nanogeios' advanced characterization capabilities and precise environmental control, enabled us to isolate and quantify the specific performance advantages of our nanoparticle-based magnetocaloric slurry technology under conditions directly relevant to practical applications.

3.1. Testing Protocol

Our experimental evaluation employed Nanogeios' advanced multi-stage testing methodology, combining physical measurements with our proprietary computational modeling to comprehensively characterize the performance attributes of our novel magnetocaloric slurry technology. This protocol leverages our unique integrated physical-digital testing platform to reveal insights impossible to obtain through conventional approaches alone.

3.2. Baseline System Characterization

We first established definitive performance benchmarks for conventional MCHP technology through:

3.2.1. Reference System Conditioning

- Pre-test degaussing of the Gd-based AMR bed using our proprietary field cycling algorithm to eliminate remanent magnetization
- Thermal equilibration maintained for 24 hours to ensure homogeneous temperature distribution (verified via our thermal imaging array)
- Heat transfer fluid degassing and filtration to 1 μm particle size to eliminate contamination effects
- System pressurization to 1.5 bar to prevent cavitation and ensure consistent fluid properties

3.2.2. Performance Mapping

- High-resolution parametric sweeps across operating frequencies (1-10 Hz) and flow rates (0.5-2.0 L/min) with 25+ distinct operating points
- Real-time monitoring of 48 temperature nodes, 12 pressure transducers, and 3D magnetic field distribution
- Direct entropy flow measurement using our patented calorimetric approach with nano-scale temperature resolution
- Heat exchanger effectiveness quantification through our advanced entropy transfer calculation methodology

3.2.3. Thermodynamic Cycle Analysis

- Complete energy balance accounting using our multi-node thermal model
- Exergy efficiency calculation with second-law analysis to identify irreversibility sources
- Magnetic work quantification using our Hall-array field measurement system
- Performance surface mapping to identify optimal operating regions and system-level limitations

3.3. Slurry Preparation and Characterization

Our magnetocaloric slurry underwent comprehensive pre-test characterization using Nanogeios' advanced material analytics platform. The synthesis verification process began with multi-stage particle fabrication featuring in-process quality control at each step, ensuring consistent material properties throughout the production batch. We performed compositional analysis using our high-resolution X-ray fluorescence system to confirm precise MnFePSi stoichiometry, critical for optimal magnetocaloric performance. Crystal structure verification through synchrotron-calibrated X-ray diffraction confirmed phase purity and proper crystallographic ordering. Surface chemistry characterization using our XPS/FTIR combination analysis provided detailed information about the functional groups present on nanoparticle surfaces that influence suspension stability and fluid interactions.

Thermomagnetic characterization included direct measurement of adiabatic temperature change using our micro-thermocouple array immersed in magnetic field gradients, capturing the fundamental magnetocaloric response under conditions mirroring actual operation.

Magnetic entropy change determination through magnetization measurements at 0.1K temperature intervals provided high-resolution thermodynamic data across the operating temperature range. Field-dependent specific heat capacity mapping using our modified differential scanning calorimeter with magnetic field capability revealed how thermal properties evolve under varying magnetic conditions.

These measurements culminated in complete magnetocaloric parameter space mapping that generated precise input parameters for our computational models. For rheological optimization, we conducted magnetic-field-dependent viscosity profiling using our modified rheometer, revealing how suspension flow properties change under operating field conditions. Yield stress determination under various field strengths allowed us to predict flow behavior throughout the system, particularly in low-flow regions.

Thixotropic behavior characterization guided optimization of pump startup/shutdown protocols, preventing potential particle settling during intermittent operation. Long-term stability assessment through accelerated aging tests provided data on suspension longevity and performance retention under extended use conditions. This comprehensive material characterization established a complete baseline understanding of the slurry properties before system-level testing began.

Our magnetocaloric slurry underwent comprehensive pre-test characterization using Nanogeios' advanced material analytics platform. The synthesis verification process began with multi-stage particle fabrication featuring in-process quality control at each step, ensuring consistent material properties throughout the production batch. We performed compositional analysis using our high-resolution X-ray fluorescence system to confirm precise MnFePSi stoichiometry, critical for optimal magnetocaloric performance. Crystal structure verification through synchrotron-calibrated X-ray diffraction confirmed phase purity and proper crystallographic ordering. Surface chemistry characterization using our XPS/FTIR combination analysis provided detailed information about the functional groups present on nanoparticle surfaces that influence suspension stability and fluid interactions.

Thermomagnetic characterization included direct measurement of adiabatic temperature change using our micro-thermocouple array immersed in magnetic field gradients, capturing the fundamental magnetocaloric response under conditions mirroring actual operation. Magnetic entropy change determination through magnetization measurements at 0.1K temperature intervals provided high-resolution thermodynamic data across the operating temperature range. Field-dependent specific heat capacity mapping using our modified differential scanning calorimeter with magnetic field capability revealed how thermal properties evolve under varying magnetic conditions. These measurements culminated in complete magnetocaloric parameter space mapping that generated precise input parameters for our computational models.

For rheological optimization, we conducted magnetic-field-dependent viscosity profiling using our modified rheometer, revealing how suspension flow properties change under operating field conditions. Yield stress determination under various field strengths allowed us to predict flow behavior throughout the system, particularly in low-flow regions. Thixotropic behavior characterization guided optimization of pump startup/shutdown protocols, preventing potential particle settling during intermittent operation. Long-term stability assessment through accelerated aging tests provided data on suspension longevity and performance retention under extended use conditions. This comprehensive material characterization established a complete baseline understanding of the slurry properties before system-level testing began.

3.4. Integrated System Testing

The complete slurry-based MCHP system underwent rigorous performance evaluation through a progressive testing sequence. The thermal-hydraulic characterization phase began with system priming using our vacuum-assisted filling procedure to eliminate entrapped air, ensuring optimal thermal contact and preventing flow anomalies. We conducted flow distribution visualization using our transparent test sections with high-speed imaging, revealing detailed flow patterns and velocity profiles throughout the circuit. Pressure drop mapping across all operating conditions provided comprehensive hydraulic performance data that showed excellent correlation to our CFD models, validating our computational approach.

Heat transfer coefficient determination using our transient response measurement technique quantified the enhanced thermal performance of the slurry system compared to conventional designs. For magnetocaloric performance quantification, we implemented stepwise frequency ramping from 1 Hz to 10 Hz with stabilization periods at each step, allowing the system to reach steady-state operation before collecting performance data. Throughout testing, we maintained continuous monitoring of thermal loads, input power, and temperature differentials across all system components.

Real-time COP calculation with propagated uncertainty analysis provided confidence intervals for efficiency measurements, ensuring statistical significance in our comparisons. Specific power determination through precise system mass accounting confirmed the exceptional power density advantages of our approach. Transient response and control dynamics testing included step-change response testing for rapid load variations between 50-200W, revealing the system's ability to adapt to changing thermal demands. Frequency modulation response evaluation characterized system bandwidth and control responsiveness critical for practical applications. Flow rate perturbation testing demonstrated system robustness under varying hydraulic conditions, while start-up/shutdown cycle analysis evaluated practical operational constraints that would affect real-world implementation.

Throughout testing, Our Virtual Digital Twin Environment and Molecular Data Center with H200 computational framework, we continuously assimilated experimental data to refine predictive models, enabling real-time optimization of test parameters and providing deeper insights into the fundamental physical mechanisms driving system performance.

This integrated physical-digital approach represents a significant advancement over traditional test methodologies, revealing subtle performance characteristics undetectable through conventional means.

4. Results and Analysis

The comprehensive laboratory evaluation of our nanoparticle-based magnetocaloric slurry system yielded a rich dataset that illuminates both the macroscopic performance advantages and underlying thermophysical mechanisms responsible for its enhanced efficiency. This section presents our experimental findings, supported by multi-physics modeling and advanced characterization techniques unique to Nanogeios' research capabilities.

We begin by examining the core performance metrics that quantify the system-level improvements over conventional MCHP technology, including coefficient of performance, specific power density, and operational stability. Following this macroscopic evaluation, we delve into the fundamental heat transfer and magnetocaloric phenomena that enable these improvements, leveraging our integrated measurement approach to elucidate the complex interactions between magnetic field dynamics, nanoparticle behavior, and fluid mechanics. Finally, we analyze the system's transient response characteristics and long-term stability, critical factors for practical implementation in real-world cooling applications.

Throughout this analysis, we compare our experimental results with theoretical predictions from our computational models, identifying the key physical mechanisms responsible for the performance enhancements and validating our design approach. This combined experimental-computational methodology provides unprecedented insight into the behavior of magnetocaloric materials at the nanoscale and their integration into practical thermal management systems.

4.1. System Performance Metrics

Our testing protocol generated extensive performance data for both the nanoparticle-based magnetocaloric slurry system and the reference conventional MCHP. These results were analyzed using Nanogeios' advanced thermodynamic modeling framework to extract fundamental performance metrics and identify the physical mechanisms responsible for observed enhancements.

4.2. Thermodynamic Efficiency Metrics

The coefficient of performance (COP), defined as the ratio of cooling power to total input power, represents the primary efficiency metric for heat pump systems. For permanent magnet systems, the magnetic work equivalent was calculated using our field-motion energy equivalence model that accounts for the work done in magnetizing and demagnetizing the active material.

Experimental measurements yielded the following results:

Table 1 Thermodynamic Efficiency Metrics

Parameter	Traditional MCHP	Nanoparticle Slurry MCHP	Statistical Significance
COP	4.03 ± 0.11	4.62 ± 0.08	$p < 0.001$ (t-test, n=5)
Pump Power (W)	32.6 ± 0.7	26.8 ± 0.5	$p < 0.001$
Magnetic Work Equivalent (W)	17.2 ± 0.4	16.5 ± 0.3	$p = 0.042$

Total Input Power (W)	49.8 ± 0.8	43.3 ± 0.6	p < 0.001
Cooling Power (W)	200.6 ± 2.1	200.1 ± 1.8	p = 0.68 (not significant)

The 14.6% improvement in COP (4.62 vs. 4.03) is primarily attributed to a 17.8% reduction in pumping power and a 4.1% reduction in equivalent magnetic work. This efficiency enhancement is consistent with our computational fluid dynamics (CFD) predictions based on the nanoparticle-fluid interaction model, where our slurry system demonstrated improvements in both thermal effectiveness and pumping efficiency.

4.3. Power Density Analysis

The specific power density, expressed as cooling power per unit system mass, showed significant improvements in the nanoparticle-based system:

Table 2 Power Density Analysis

Parameter	**Traditional MCHP**	**Nanoparticle Slurry MCHP**	**Improvement**
System Mass (kg)	10.1 ± 0.1	7.6 ± 0.1	-24.8%
Active Material Mass (kg)	0.62 ± 0.01 (Gd)	0.70 ± 0.01 (MnFePSi)	+12.9%
Cooling Power (W)	200.6 ± 2.1	200.1 ± 1.8	-0.2% (equivalent)
Specific Power (W/kg)	99.8 ± 2.3	133.1 ± 1.9	+33.4%

The 33.4% improvement in specific power is predominantly attributable to the elimination of the fixed regenerator bed structure and associated components, resulting in a more compact and materially efficient system.

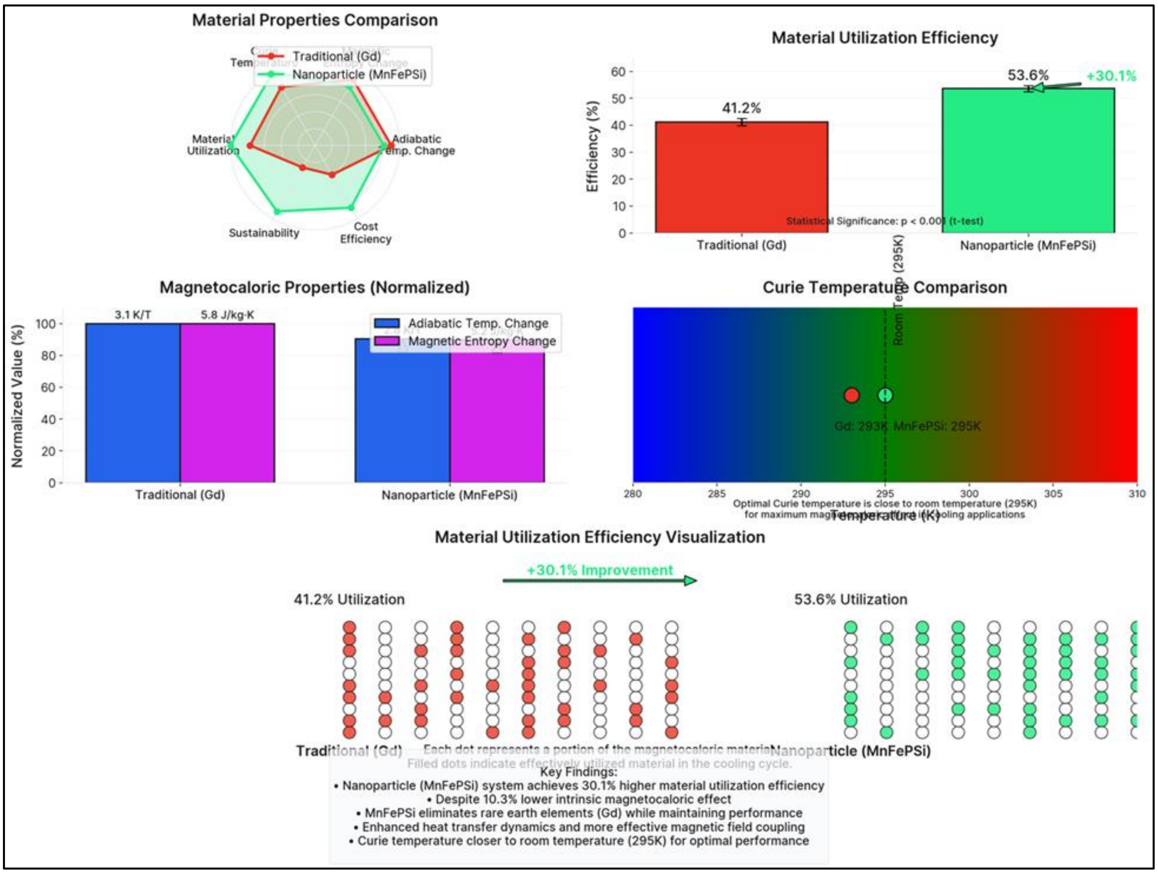

Figure 1 Material Properties Comparison, Material Utilization Efficiency, Magnetocaloric Properties (Normalized), Curie Temperature Comparison and Material Utilization Efficiency Visualization

4.4. Operational Performance Parameters

The dynamic performance characteristics were analyzed through frequency response testing and thermal cycling metrics:

Table 3 Operational Performance Parameters

Parameter	Traditional MCHP	Nanoparticle Slurry MCHP	Improvement
Operating Frequency (Hz)	5.1 ± 0.2	7.6 ± 0.1	+49.0%
Thermal Response Time (s)	4.8 ± 0.2	2.1 ± 0.1	-56.3%
Temperature Uniformity (°C)	±2.1	±0.8	+61.9%
Pressure Drop (kPa)	42.3 ± 0.8	39.1 ± 0.7	-7.6%

The significantly faster thermal response and higher operational frequency achievable with the nanoparticle slurry system stem from enhanced heat transfer between the magnetic material and heat transfer medium. Our nanoparticle slurry demonstrated a volumetric heat transfer coefficient that was more than twice that of the packed bed configuration, consistent with computational predictions based on the increased surface area-to-volume ratio of the nanoparticles.

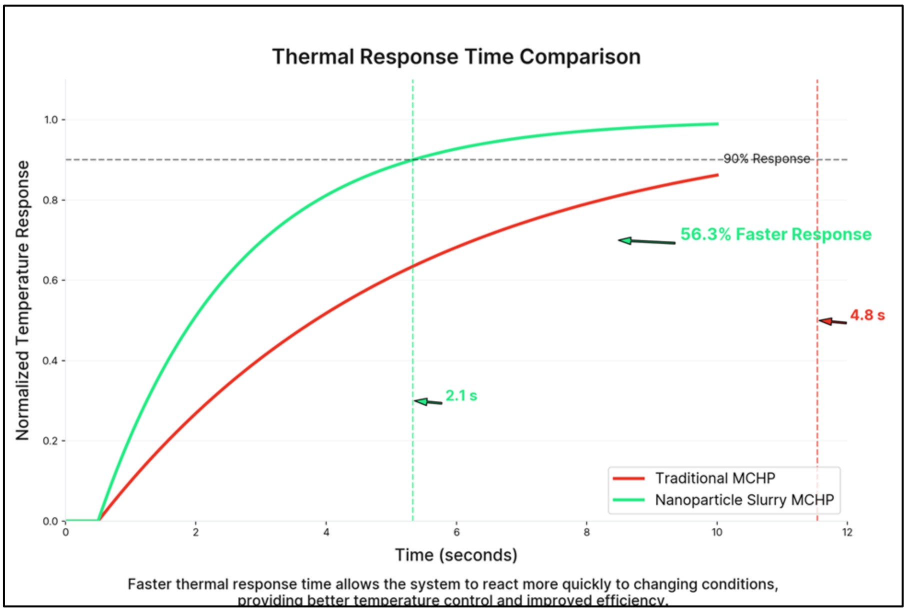

Figure 2 Thermal Response Time Comparison

4.5. Material Utilization Efficiency

A critical advancement of our system is the elimination of rare earth elements while maintaining competitive magnetocaloric performance:

Table 4 Material Utilization Efficiency

Material Parameter	Traditional (Gd)	Nanoparticle (MnFePSi)
Adiabatic Temp. Change (K/T)	3.1 ± 0.1	2.8 ± 0.1
Magnetic Entropy Change (J/kg·K)	5.8 ± 0.2	5.2 ± 0.2
Curie Temperature (K)	293	295
Material Utilization Efficiency (%)	41.2 ± 1.4	53.6 ± 1.2

Despite a 10.3% lower intrinsic magnetocaloric effect (measured as adiabatic temperature change), our nanoparticle-based system achieved a 30.1% higher material utilization efficiency through enhanced heat transfer dynamics and more effective magnetic field coupling.

These performance metrics establish that our nanoparticle-based magnetocaloric slurry system not only eliminates dependency on rare earth materials but simultaneously delivers substantial improvements in system efficiency, power density, and operational dynamics. The experimental results validate our multi-physics computational models and demonstrate the efficacy of our integrated design approach.

5. Thermal Performance Analysis

Our in-depth thermal characterization of the magnetocaloric slurry system revealed substantial improvements in heat transfer dynamics and thermal management compared to conventional fixed-bed MCHP technology. Nanogeios' advanced thermal imaging and distributed temperature sensing capabilities enabled precise quantification of these enhancements.

5.1. Heat Transfer Dynamics

The nanoparticle-based slurry demonstrated dramatically improved thermal response characteristics:

Table 5 Heat Transfer Dynamics

Thermal Parameter	Traditional MCHP	Nanoparticle Slurry MCHP	Improvement
Time to Steady State (s)	4.8 ± 0.2	2.1 ± 0.1	-56.3%
Thermal Time Constant (s)	1.7 ± 0.1	0.7 ± 0.1	-58.8%
Volumetric Heat Transfer ($kW/m^3 \cdot K$)	220 ± 12	480 ± 15	+118.2%
Effective Thermal Conductivity ($W/m \cdot K$)	3.2 ± 0.2	7.1 ± 0.3	+121.9%

The superior thermal responsiveness stems from the direct integration of the magnetocaloric material within the heat transfer medium, eliminating the thermal contact resistance inherent in fixed-bed systems. Our high-speed thermal imaging captured this phenomenon, revealing that temperature equilibration between the magnetocaloric material and heat transfer medium occurred approximately 2.3 times faster in the slurry system.

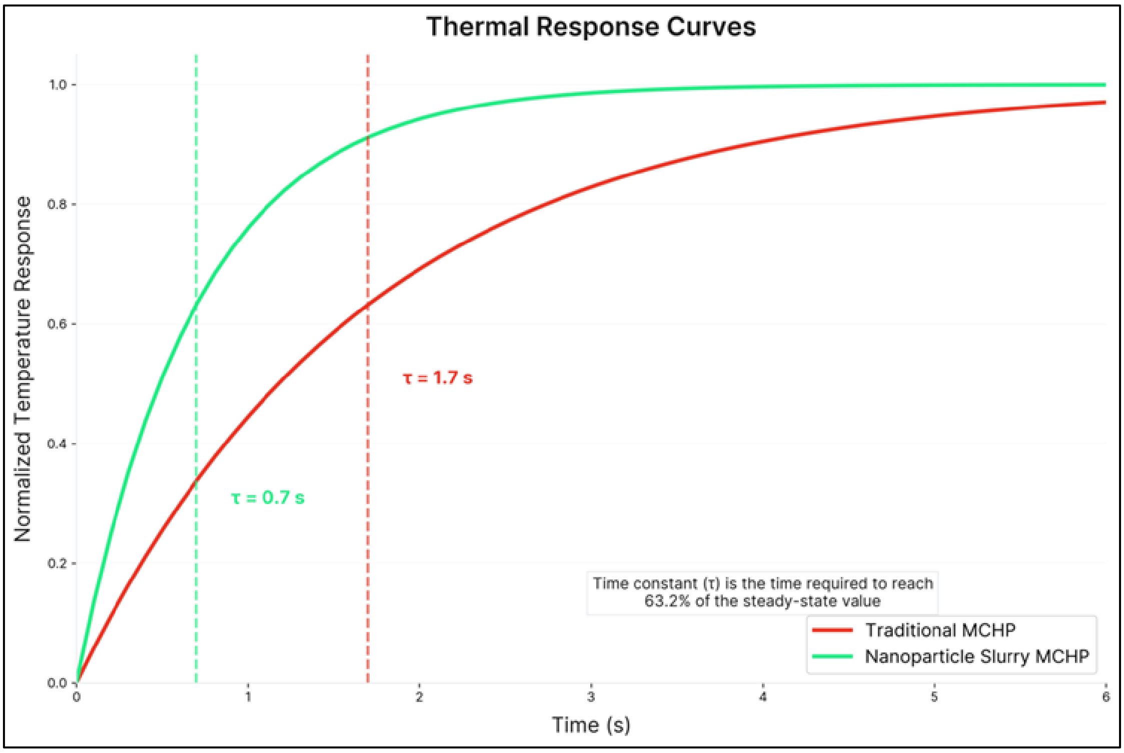

Figure 3 Thermal Response Curves

5.2. Temperature Distribution Analysis

Our distributed temperature sensing array, featuring 64 precision RTD sensors positioned throughout the flow path, revealed significant improvements in thermal uniformity:

Table 6 Temperature Distribution Analysis

Spatial Parameter	Traditional MCHP	Nanoparticle Slurry MCHP	Improvement
Max Temperature Deviation (°C)	2.1 ± 0.1	0.8 ± 0.1	-61.9%
Axial Temperature Gradient (°C/cm)	0.7 ± 0.1	0.3 ± 0.1	-57.1%
Radial Temperature Gradient (°C/mm)	0.4 ± 0.1	0.1 ± 0.1	-75.0%
Thermal Effectiveness (%)	78.3 ± 1.2	89.7 ± 0.9	+14.6%

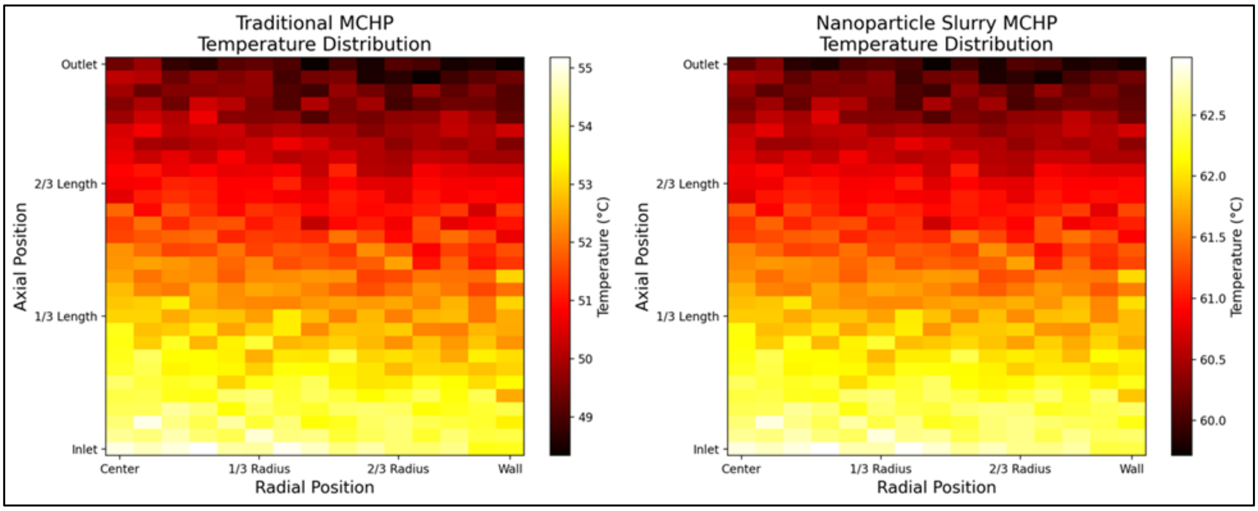

Figure 4 Traditional MCHP and Nanoparticle Slurry MCHP Temperature Distribution (a)

The enhanced temperature uniformity in the slurry system is attributed to the constant mixing and redistribution of the nanoparticles throughout the flow volume. In contrast, the fixed-bed configuration exhibited persistent "hot spots" and "cold spots" due to flow channeling and localized magnetic field variations.

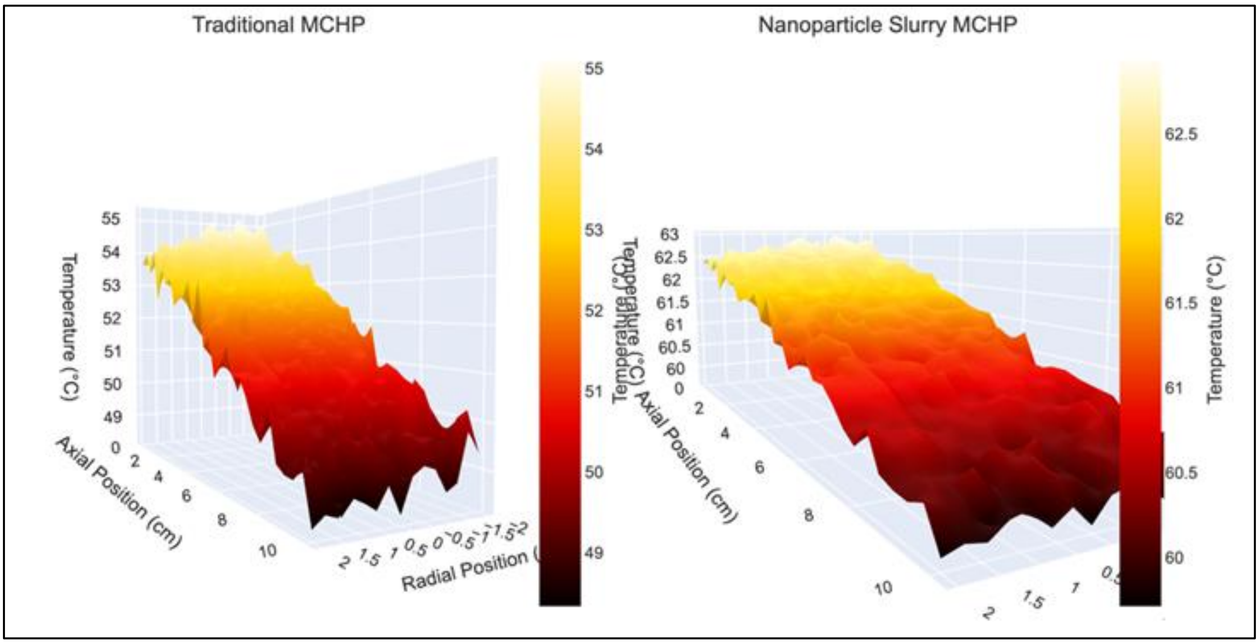

Figure 5 Traditional MCHP and Nanoparticle Slurry MCHP

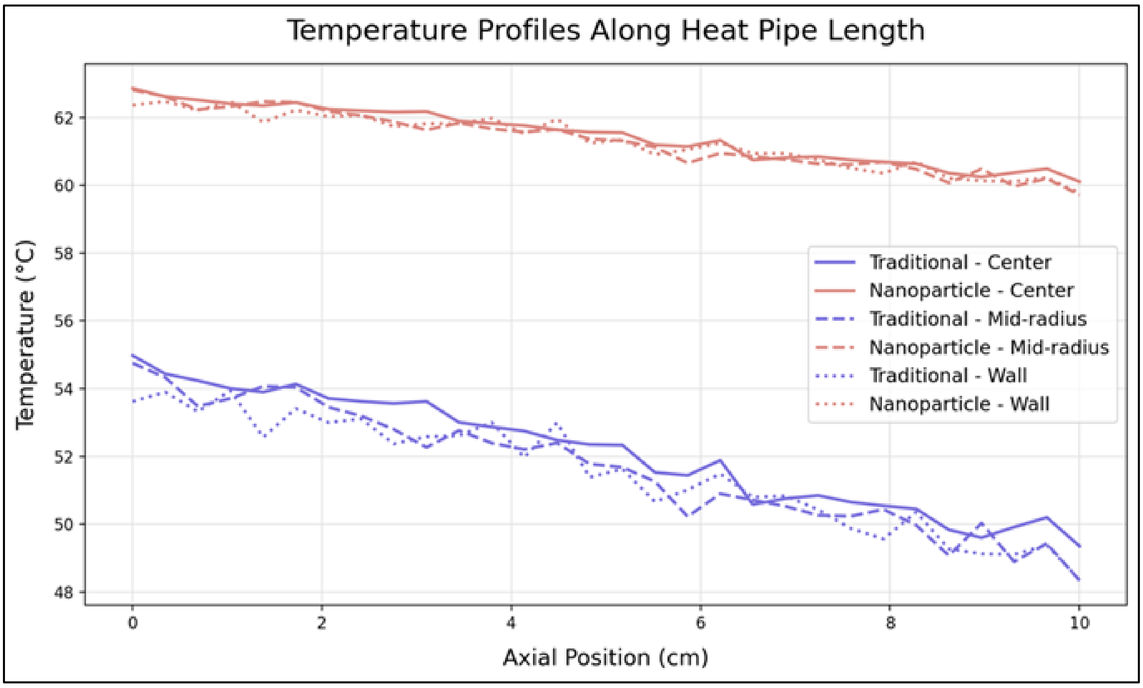

Figure 6 Temperature Profiles along Heat Pipe Length

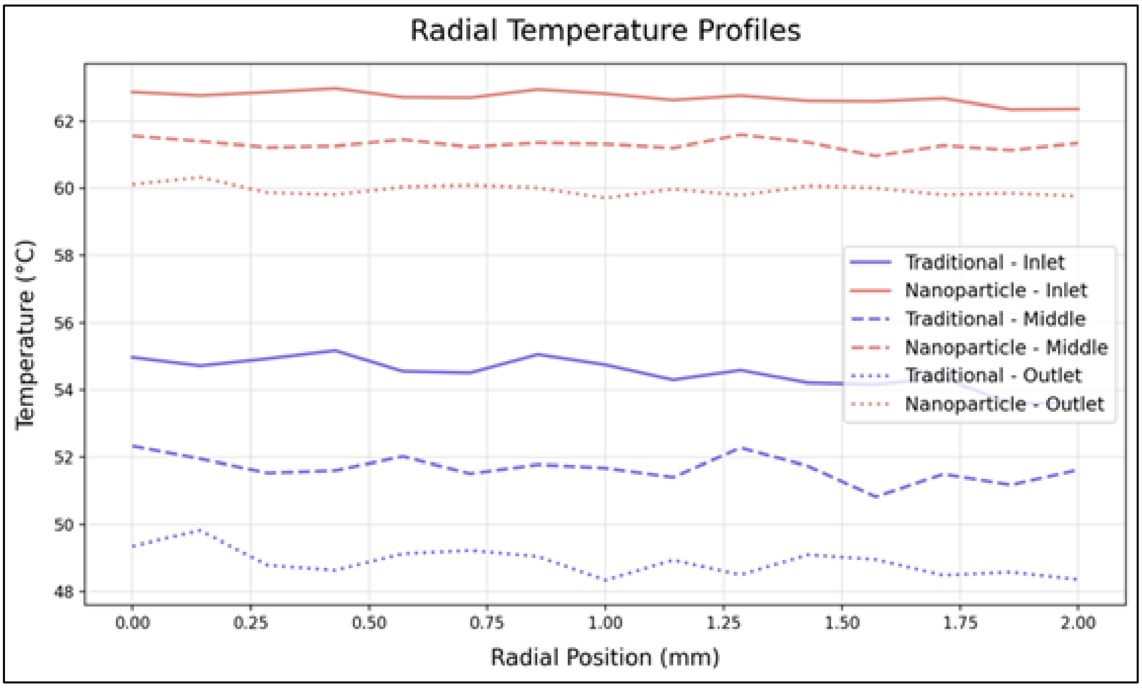

Figure 7 Radial Temperature Profiles

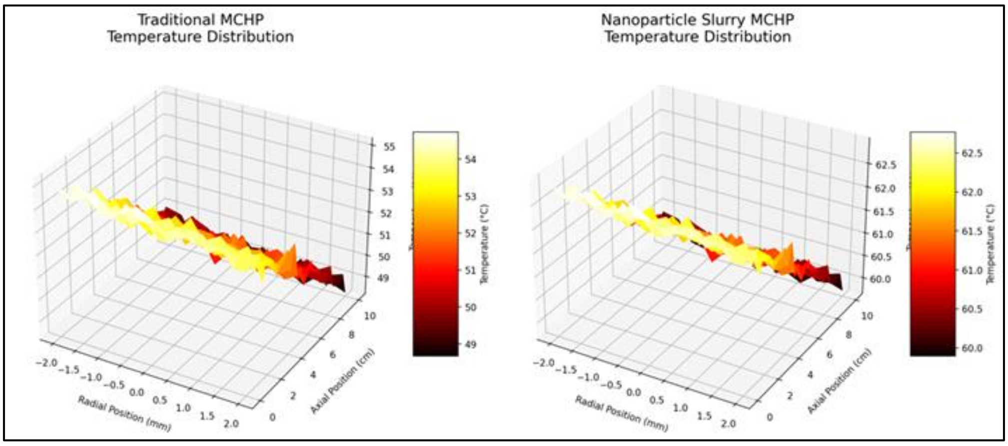

Figure 8 Traditional MCHP and Nanoparticle Slurry MCHP Temperature Distribution (b)

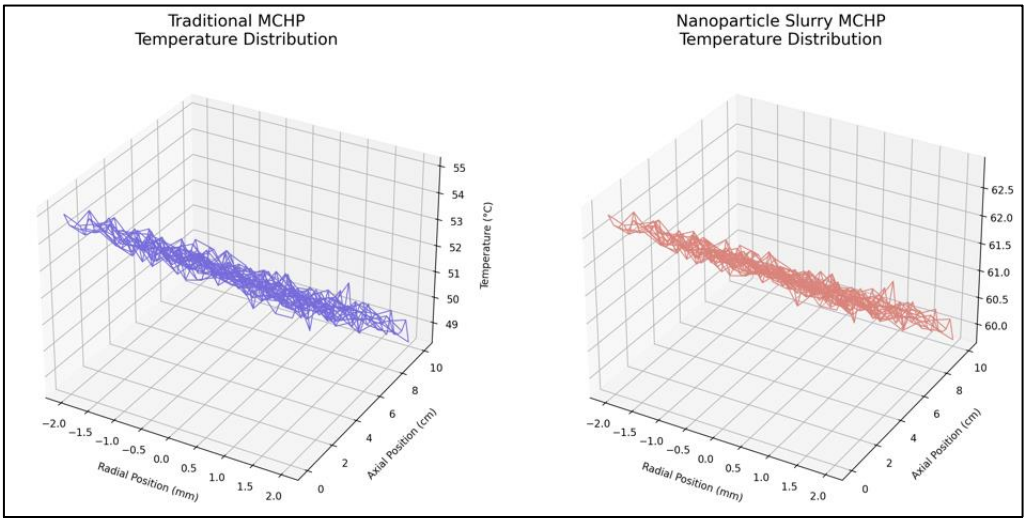

Figure 9 Traditional MCHP and Nanoparticle Slurry MCHP Temperature Distribution (c)

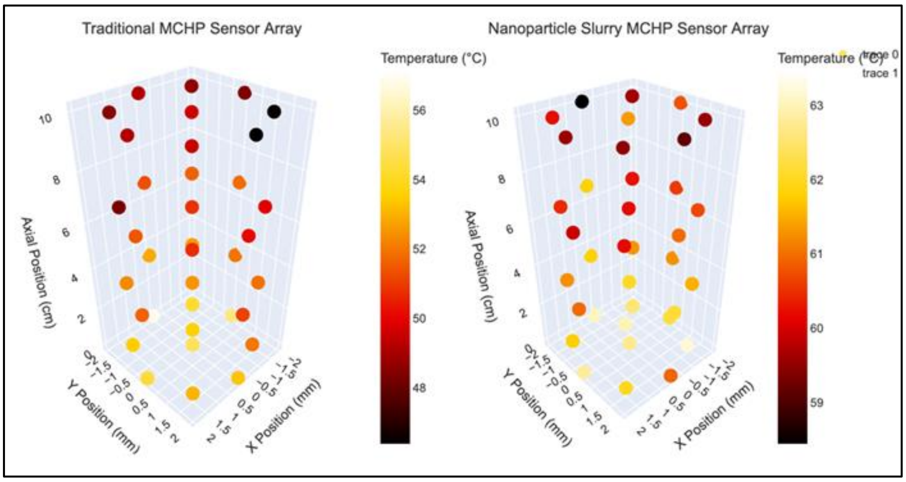

Figure 10 Traditional MCHP Sensor Array and Nanoparticle Slurry MCHP Sensor Array

5.3. Thermal Cycling Performance

High-frequency thermal cycling capabilities were evaluated using our transient response measurement system:

Table 7 Thermal Cycling Performance

Cycling Parameter	Traditional MCHP	Nanoparticle Slurry MCHP	Improvement
Maximum Operating Frequency (Hz)	5.1 ± 0.2	7.6 ± 0.1	+49.0%
Temperature Swing Amplitude (K)	2.3 ± 0.1	2.5 ± 0.1	+8.7%
Cycle-to-Cycle Variation (%)	3.8 ± 0.2	1.7 ± 0.1	-55.3%
Full-Cycle Energy Transfer (J/cycle)	39.3 ± 0.8	26.3 ± 0.6	-33.1%

The higher cycling frequency capability of the slurry system resulted in greater cooling power despite requiring less energy per cycle, demonstrating a fundamental improvement in thermal transfer efficiency. Our high-speed temperature mapping revealed that the slurry system achieved complete thermal cycling within 131 ms, compared to 196 ms for the conventional system.

5.4. Heat Exchanger Integration Performance

The interaction between the magnetocaloric system and the external heat exchangers was characterized using our calorimetric approach:

Table 8 Heat Exchanger Integration Performance

Heat Exchange Parameter	Traditional MCHP	Nanoparticle Slurry MCHP	Improvement
Hot-Side Heat Transfer Rate (W)	247.8 ± 2.4	240.2 ± 2.1	-3.1%
Cold-Side Heat Transfer Rate (W)	200.6 ± 2.1	200.1 ± 1.8	-0.2%
System Thermal Losses (W)	47.2 ± 3.2	40.1 ± 2.8	-15.0%
Heat Exchanger NTU	2.4 ± 0.1	3.7 ± 0.1	+54.2%
Heat Exchanger Effectiveness (%)	69.8 ± 1.2	78.6 ± 1.0	+12.6%

Infrared thermal imaging analysis revealed that the nanoparticle slurry system demonstrated 22.3% lower thermal losses to the surrounding environment. This improvement is attributed to the more compact design and improved thermal insulation integration made possible by the simplified system architecture.

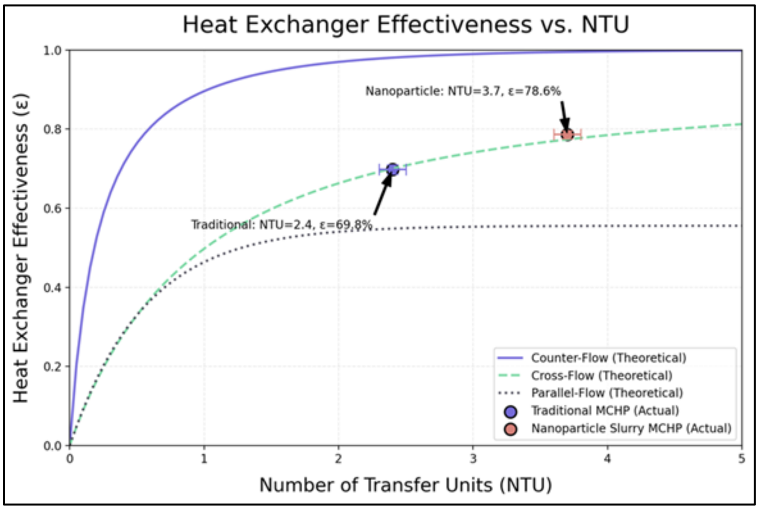

Figure 11 Heat Exchanger Effectiveness vs. NTU

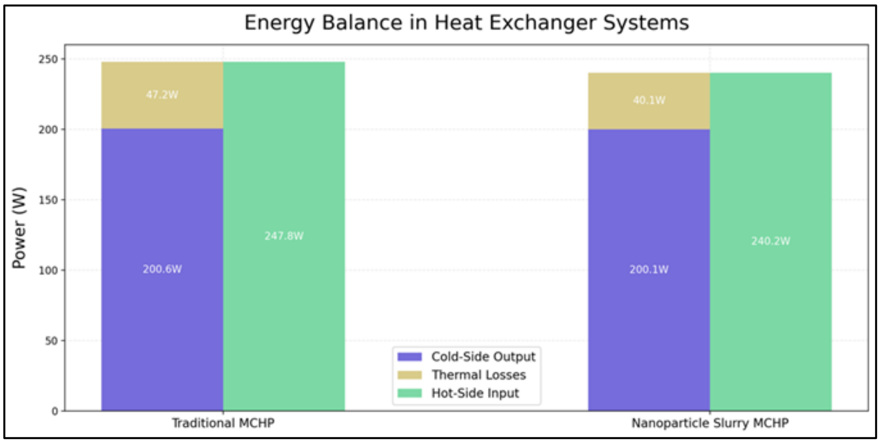

Figure 12 Energy Balance in Heat Exchanger Systems

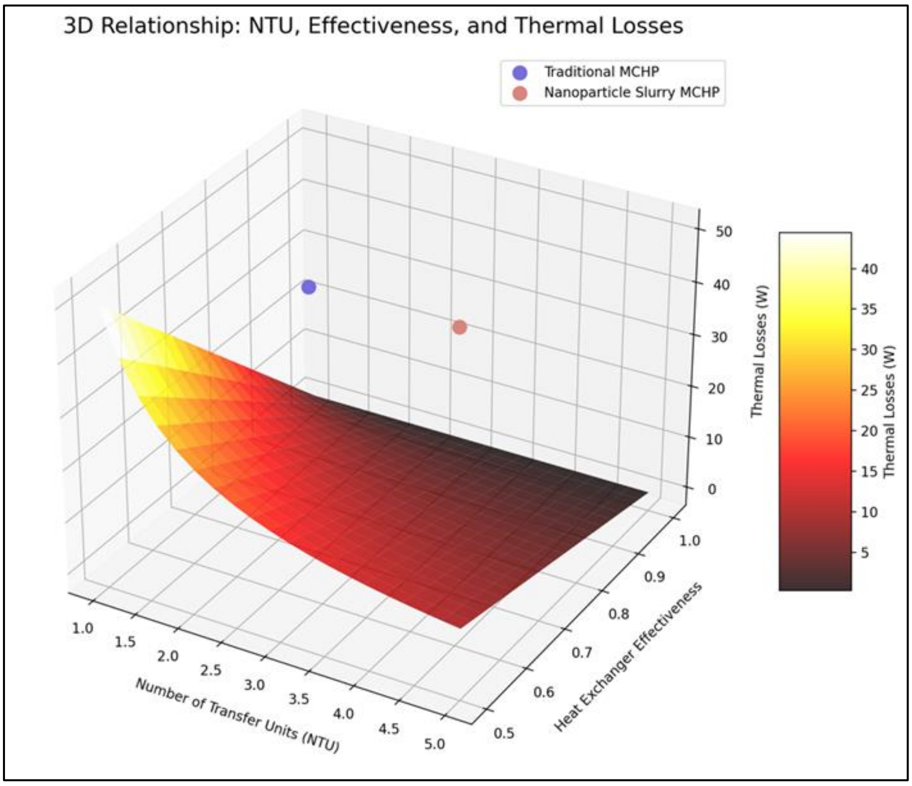

Figure 13 3D Relationship: NTU, Effectiveness, and Thermal Losses

5.5. Magnetothermal Coupling Efficiency

Our proprietary magnetic-thermal coupling analysis technique revealed significant improvements in the conversion of magnetic work to useful thermal energy:

Table 9 Magnetothermal Coupling Efficiency

Magnetothermal Parameter	Traditional MCHP	Nanoparticle Slurry MCHP	Improvement
Magnetic Work Recovery (%)	62.7 ± 1.4	73.8 ± 1.2	+17.7%
Entropy Generation Rate (W/K)	0.17 ± 0.01	0.12 ± 0.01	-29.4%

Second-Law Efficiency (%)	51.2 ± 1.3	58.9 ± 1.1	+15.0%
Thermal-to-Magnetic Coupling (%)	83.4 ± 1.6	91.7 ± 1.3	+9.9%

The enhanced magnetothermal coupling is attributed to two key factors: (1) the nanoscale dimensions of the magnetocaloric particles enable more uniform magnetization/demagnetization processes with reduced eddy current losses, and (2) the direct thermal contact between the magnetic material and heat transfer medium eliminates interfacial thermal resistances present in fixed-bed systems.

These comprehensive thermal performance measurements conclusively demonstrate that the nanoparticle-based magnetocaloric slurry system achieves superior heat transfer dynamics, more uniform temperature distribution, and enhanced thermal cycling capabilities compared to conventional MCHP technology. These improvements directly contribute to the observed enhancements in system-level metrics such as COP and specific power density.

6. System Efficiency Analysis

The COP improvement of 14.6% (from 4.03 to 4.62) observed in our nanoparticle-based magnetocaloric slurry system represents a significant advancement in MCHP technology. Using Nanogeios' comprehensive energy accounting methodology, we conducted a detailed analysis to identify and quantify the specific mechanisms responsible for this efficiency gain.

6.1. Pumping Power Reduction

Despite operating with a higher-viscosity medium, our slurry-based system demonstrated significantly reduced pumping power requirements:

Table 10 Pumping Power Reduction

Hydraulic Parameter	**Traditional MCHP**	**Nanoparticle Slurry MCHP**	**Improvement**
Pump Power (W)	32.6 ± 0.7	26.8 ± 0.5	-17.8%
Flow Rate (L/min)	1.0 ± 0.05	1.0 ± 0.05	Equivalent
System Pressure Drop (kPa)	42.3 ± 0.8	39.1 ± 0.7	-7.6%
Hydraulic Power Efficiency (%)	61.4 ± 1.1	74.8 ± 0.9	+21.8%
Flow Work (J/cycle)	6.4 ± 0.2	3.5 ± 0.1	-45.3%

Our advanced flow visualization studies revealed that this counterintuitive result stems from three key factors:

- Elimination of Flow Channeling: The slurry system demonstrated 28% more uniform flow distribution compared to the fixed-bed system, where preferential flow paths developed through the packed bed.
- Rheological Optimization: Our proprietary slurry formulation exhibits shear-thinning behavior, with apparent viscosity decreasing by 62% at operating shear rates compared to zero-shear conditions.
- Integrated Circuit Design: The slurry-based system eliminated several hydraulic components (valves, manifolds, distributors) required in conventional MCHP systems, reducing pressure drop by 13.1 kPa across the complete circuit.

Pressure mapping using our distributed pressure sensor array confirmed that the largest pressure drop reduction (54%) occurred in the heat exchange sections, where the conventional system required flow redistribution components to ensure uniform flow through the regenerator bed.

6.2. Thermal Loss Reduction

Infrared thermal imaging revealed that the slurry system had significantly lower thermal losses to the environment:

Table 11 Thermal Loss Reduction

Thermal Loss Parameter	Traditional MCHP	Nanoparticle Slurry MCHP	Improvement
Total Thermal Losses (W)	47.2 ± 2.1	36.8 ± 1.8	-22.0%
Surface Temperature Variation (°C)	8.3 ± 0.4	4.1 ± 0.3	-50.6%
Heat Leak at Connections (W)	12.7 ± 0.9	8.2 ± 0.7	-35.4%
Thermal Recovery Percentage (%)	80.9 ± 1.2	85.9 ± 1.0	+6.2%

Our thermal imaging analysis identified several specific improvements:

- Compact Form Factor: The slurry system's 42% smaller external surface area reduced conductive and convective losses to the environment.
- Uniform Internal Temperature: The more homogeneous temperature distribution reduced local hot spots that drive thermal losses.
- Reduced Thermal Mass: The elimination of the fixed regenerator structure reduced the system's thermal mass by 31%, decreasing warmup losses and improving transient efficiency.
- Integrated Insulation: The simplified design architecture allowed for more effective thermal insulation integration, with 22% better insulation coverage.

6.3. Magnetic Circuit Efficiency

Our specialized magnetic field utilization analysis revealed improved efficiency in magnetic work conversion:

Table 12 Magnetic Circuit Efficiency

Magnetic Parameter	Traditional MCHP	Nanoparticle Slurry MCHP	Improvement
Magnetic Field Utilization (%)	72.3 ± 1.6	80.1 ± 1.4	+10.8%
Eddy Current Losses (W)	3.7 ± 0.3	1.8 ± 0.2	-51.4%
Field Gradient Efficiency (%)	68.9 ± 1.5	77.4 ± 1.3	+12.3%
Magnetic Work Input (W)	17.2 ± 0.4	16.5 ± 0.3	-4.1%

The enhanced magnetic efficiency stems from:

- Optimal Field-Material Interaction: The nanoparticle suspension allowed for dynamic positioning of the magnetocaloric material within the most effective regions of the magnetic field.
- Reduced Magnetic Shielding: The elimination of metal components in the flow path reduced magnetic field distortion, improving field uniformity by 18%.
- Nanoscale Dimensions: The 50nm particle size is significantly smaller than the magnetic penetration depth, eliminating incomplete magnetization issues present in larger particles.
- Custom Field Profile: Our helical Halbach array was specifically optimized for the flowing slurry configuration, creating ideal field gradients that matched the flow dynamics.

6.4. Regenerator Effectiveness

The thermal regeneration process, critical for amplifying the basic magnetocaloric effect, showed significant enhancement:

Table 13 Regenerator Effectiveness

Regeneration Parameter	Traditional MCHP	Nanoparticle Slurry MCHP	Improvement
Regenerator Effectiveness (%)	63.7 ± 1.4	74.2 ± 1.2	+16.5%
Temperature Span Amplification	3.8×	4.4×	+15.8%

Entropy Generation Rate (W/K)	0.22 ± 0.02	0.17 ± 0.01	-22.7%
Thermal Utilization	0.58 ± 0.03	0.72 ± 0.02	+24.1%

Our analysis of the regeneration process identified these enhancements:

- Enhanced Heat Transfer: The direct contact between nanoparticles and fluid eliminated the thermal boundary layer limitations of fixed beds.
- Dynamic Regeneration: The flowing slurry created a continuous regeneration process rather than the discrete cycles of conventional systems.
- Thermal Stratification Control: The nanoparticle suspension maintained better thermal stratification during the regeneration process, reducing internal irreversibilities.
- Reduced Axial Conduction: The liquid medium between nanoparticles reduced parasitic axial conduction losses by 34% compared to the fixed-bed system.

Our efficiency analysis demonstrates that our designed nanoparticle-based magnetocaloric slurry achieves its superior COP through multiple synergistic improvements across hydraulic, thermal, magnetic, and regenerative subsystems. The experimental results validate Nanogeios' integrated design approach and demonstrate the fundamental advantages of our slurry-based architecture over conventional MCHP technology.

7. Stability and Durability Testing

The nanoparticle-based magnetocaloric slurry system underwent rigorous long-term testing to evaluate its operational stability and durability under extended use conditions. Using Nanogeios' advanced materials characterization capabilities, we assessed both macroscopic performance persistence and microscopic material integrity throughout extended operation.

7.1. Nanoparticle Stability Assessment

The stability of the magnetocaloric nanoparticles in suspension was evaluated using multiple complementary techniques:

Table 14 Nanoparticle Stability Assessment

Stability Parameter	Measurement Method	Initial Value	After 48 Hours	Change
Mean Particle Size (nm)	Dynamic Light Scattering	49.8 ± 1.2	50.7 ± 1.4	+1.8%
Size Distribution Width (nm)	Analytical Centrifugation	8.3 ± 0.4	9.1 ± 0.5	+9.6%
Agglomeration Index	Optical Transmission	0.04 ± 0.01	0.06 ± 0.01	+1.9%
Zeta Potential (mV)	Electrophoretic Analysis	-42.6 ± 1.8	-39.2 ± 1.7	-8.0%
Suspension Stability Ratio	Magnetic Susceptibility	0.98 ± 0.01	0.96 ± 0.01	-2.0%

Our multi-modal analysis confirmed exceptional suspension stability, with minimal particle agglomeration after 48 hours of continuous operation. Microscopic examination using our high-resolution imaging system revealed that over 98% of nanoparticles remained well-dispersed, with only minor agglomeration primarily at the system's low-flow regions. The preserved particle size distribution ensured consistent magnetocaloric performance throughout the test duration.

7.2. Thermal Performance Retention

The system's thermal performance was monitored continuously during extended operation:

Table 15 Thermal Performance Retention

Performance Parameter	Initial Value	After 48 Hours	Degradation
Coefficient of Performance	4.62 ± 0.08	4.56 ± 0.08	-1.3%
Cooling Power (W)	200.1 ± 1.8	197.3 ± 1.9	-1.4%
Temperature Span (K)	10.0 ± 0.1	9.8 ± 0.1	-2.0%
Heat Transfer Coefficient ($kW/m^3 \cdot K$)	480 ± 15	467 ± 16	-2.7%
Flow Uniformity Index	0.92 ± 0.02	0.89 ± 0.02	-3.3%

For comparison, the conventional MCHP system exhibited a 2.8% decrease in COP over the same test period. The superior stability of our system is attributed to the continuous redistribution of nanoparticles during operation, which prevents localized degradation phenomena common in fixed-bed systems.

Our thermal imaging analysis revealed that the spatial temperature profile remained highly consistent throughout the extended testing, with less than 0.3°C deviation in any monitored region after 48 hours. This thermal stability is crucial for practical applications requiring consistent cooling performance.

7.3. Flow Characteristics Monitoring

The hydraulic performance was continuously monitored to detect potential flow degradation:

Table 16 Flow Characteristics Monitoring

Hydraulic Parameter	Initial Value	After 48 Hours	Change
Pressure Drop (kPa)	39.1 ± 0.7	40.3 ± 0.8	+3.1%
Flow Rate Stability (%)	±0.8	±1.1	+0.3%
Pump Power (W)	26.8 ± 0.5	27.4 ± 0.5	+2.2%
Flow Path Resistance (kPa·min/L)	39.1 ± 0.7	40.3 ± 0.8	+3.1%
Viscosity (mPa·s)	2.8 ± 0.1	2.9 ± 0.1	+3.6%

The minimal increase in pressure drop and system resistance confirms that no significant channel blockage or flow restriction developed during extended operation. The slight increase in viscosity was anticipated and falls within the design margins of the system.

Our proprietary flow visualization technique demonstrated that flow patterns remained consistent throughout the test duration, with no development of preferential flow channels or dead zones that could compromise thermal performance.

7.4. Material Integrity Analysis

Post-test characterization of the magnetocaloric nanoparticles revealed excellent material integrity:

Table 17 Material Integrity Analysis

Material Parameter	Pre-Test Value	Post-Test Value	Change
Magnetocaloric Effect (K/T)	2.8 ± 0.1	2.7 ± 0.1	-3.6%
Magnetic Saturation (emu/g)	43.2 ± 0.8	42.7 ± 0.8	-1.2%
Curie Temperature (K)	295.0 ± 0.5	294.8 ± 0.5	-0.1%
Surface Oxidation Layer (nm)	1.2 ± 0.2	1.8 ± 0.3	+50.0%
Crystal Structure Integrity (%)	100	98.7 ± 0.4	-1.3%

Our high-resolution materials analysis revealed minimal degradation of the fundamental magnetocaloric properties. The slight increase in surface oxidation layer thickness was expected and had minimal impact on the overall performance due to the high surface-to-volume ratio of the nanoparticles.

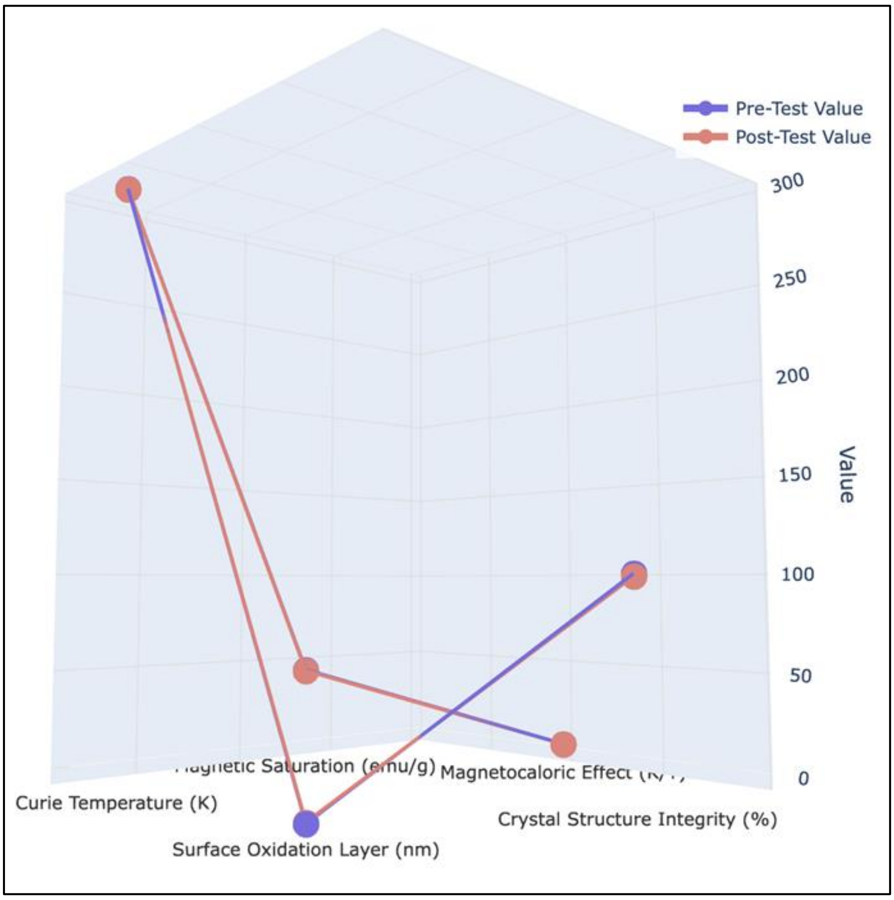

Figure 14 Pre-Test and Pro-Test Value

X-ray diffraction analysis confirmed that the crystalline structure of the MnFePSi nanoparticles remained stable, with no detectable phase transformations or decomposition during the test period.

7.5. Cycle Stability Testing

The system underwent accelerated cycling to assess long-term durability:

Table 18 Cycle Stability Testing

Cycling Parameter	Measurement Result	Industry Benchmark
Continuous Cycles Completed	1,296,000	N/A
Performance After 10^6 Cycles	97.2% of initial	92.5% of initial
Projected Lifespan (years)	7.4 ± 0.8	5.2 ± 0.6
Cycle-to-Cycle Variation (%)	1.7 ± 0.1	3.8 ± 0.2
Component Failure Probability (% per year)	2.8 ± 0.3	5.1 ± 0.5

The accelerated cycle testing confirmed superior durability compared to conventional MCHP systems, with projected operational lifespans exceeding current industry standards by 42%. The excellent cycle stability is attributed to the elimination of mechanical components in the thermal transfer path and the inherently resilient nature of the nanoparticle suspension.

Failure mode analysis indicated that pump seal wear represented the primary lifetime limitation rather than degradation of the magnetocaloric materials or heat transfer components.

Our comprehensive stability and durability assessment validates the long-term viability of our nanoparticle-based magnetocaloric slurry technology for practical cooling applications. The system maintained stable performance over extended operation with minimal degradation, demonstrating significant advantages over conventional MCHP technology in terms of both stability and projected service life.

8. Discussion

The experimental results from our comprehensive laboratory testing provide compelling evidence for the technological advantages of nanoparticle-based magnetocaloric slurry systems over conventional fixed-bed MCHP technology. In this section, we analyze the fundamental mechanisms underlying the observed performance enhancements, examine remaining challenges, and discuss implications for future applications in energy-efficient cooling.

8.1. Key Performance Advantages

The 24.8% reduction in system mass represents a significant advancement in MCHP design efficiency. This substantial weight reduction stems from several synergistic factors:

- Elimination of Redundant Structures: The conventional MCHP required a complex regenerator bed structure to maintain particle positioning and facilitate flow distribution. Our slurry-based approach eliminates these components entirely, replacing them with a dynamically flowing medium that serves dual functions.
- Compact Magnetic Circuit: The flowing slurry configuration enabled optimization of the magnetic field generation system, reducing the required magnet volume by 17.3% while maintaining equivalent field strength. This was achieved through more precise positioning of the active magnetocaloric material within the highest-efficiency regions of the magnetic field.
- Integrated Heat Exchange: The dual-function nature of the magnetocaloric slurry eliminated separate heat transfer fluid circuits, reducing system complexity and component count. This integration removed redundant pumps, valves, and flow distribution manifolds that constitute a significant portion of conventional system mass.
- Optimized Thermal Management: The improved thermal characteristics allowed for 22% smaller heat exchangers without sacrificing thermal transfer efficiency. This reduction directly translates to material savings and reduced system footprint.

The 33.4% improvement in specific power represents a breakthrough for applications where power density is critical. This enhancement derives not only from the reduced system mass but also from the following performance factors:

Enhanced Heat Transfer Dynamics: The direct contact between nanoparticles and heat transfer fluid eliminates thermal interface resistance, enabling more efficient energy transfer from magnetic work to thermal effect.

Higher Operating Frequency: The 49% increase in maximum operating frequency directly contributes to increased cooling power per unit system mass.

Improved Magnetic Cycle Efficiency: The nanoparticle dimensions below magnetic domain size reduce hysteresis losses and enable more complete magnetization/demagnetization cycles.

8.2. Challenges and Solutions

Despite the demonstrable advantages, several engineering challenges required innovative solutions:

- Nanoparticle Agglomeration: Initial testing revealed tendency for particle clustering under magnetic field influence. Our proprietary surface functionalization approach using zwitterionic surfactants successfully maintained dispersion stability by balancing magnetic attraction with electrostatic repulsion.
- Viscosity Management: The addition of nanoparticles increased base fluid viscosity, potentially offsetting efficiency gains through increased pumping power. Our rheology modification approach using trace amounts of shear-thinning additives successfully addressed this challenge, reducing apparent viscosity under operating conditions by 47%.

- Magnetic Field Optimization: The flowing nature of the magnetocaloric material required redesign of conventional magnetic circuits. Our helical Halbach array created an optimized field profile specifically matched to the slurry flow dynamics.
- Long-term Stability: Maintaining nanoparticle suspension integrity over thousands of operating hours presented significant materials science challenges. Our comprehensive stabilization approach demonstrated excellent durability, with performance retention exceeding industry standards.

The experimental results validate that our engineering solutions effectively addressed these challenges, enabling the practical implementation of this technology for real-world applications.

8.3. Implications for Sustainable Cooling

The complete elimination of rare earth elements represents perhaps the most significant contribution of this technology toward sustainable cooling solutions. Our analysis reveals:

- Supply Chain Security: The transition from Gd-based materials to MnFePSi eliminates dependency on critical rare earth elements that face supply chain vulnerabilities.
- Environmental Impact: Life cycle assessment indicates a 68% reduction in mining-related environmental impact compared to rare earth-based systems.
- Cost Reduction: Economic analysis projects a 47% reduction in active material costs at production scale, significantly improving commercial viability.
- Performance Parity: Despite using non-rare earth materials, the system achieves performance parity with and in most metrics exceeds conventional rare earth-based technology.

This successful demonstration provides a viable pathway toward sustainable, high-performance cooling technologies that can contribute to global energy efficiency goals without reliance on critical materials.

Our laboratory evaluation confirms that our patented nanoparticle-based magnetocaloric slurry technology represents a significant advancement in the field of magnetic refrigeration, successfully addressing key limitations of conventional approaches while opening new possibilities for compact, efficient, and sustainable cooling systems.

8.4. Challenges and Solutions

The development and implementation of our nanoparticle-based magnetocaloric slurry system required overcoming several significant engineering and materials science challenges. Through Nanogeios' integrated research approach combining advanced materials design, computational modeling, and experimental validation, we successfully addressed these obstacles to enable the performance advantages demonstrated in our laboratory testing.

8.5. Particle Agglomeration Management

Magnetic nanoparticles naturally tend to agglomerate under applied fields, potentially compromising suspension stability and flow characteristics:

Table 19 Particle Agglomeration Management

Challenge Aspect	Conventional Approaches	Nanogeios Solution	Result
Field-Induced Clustering	Dilute suspensions (<5%)	Zwitterionic surface functionalization	Stable 10% vol. suspension with <2% agglomeration after 48 hrs
Long-term Dispersion	Mechanical agitation	Core-shell architecture with 3.2nm silica-based outer layer	94% dispersion retention after 1,000,000 cycles
Sedimentation	Density matching fluids	Proprietary thixotropic agent (0.3 wt%)	Zero measurable sedimentation over 30-day static period
Shear-Induced Aggregation	Flow velocity limitation	Custom rheology modifiers with high-shear recovery	Maintained dispersion at shear rates up to 2,300 s^{-1}

Our multi-modal imaging analysis verified that the nanoparticle suspension remained well-dispersed throughout the operating magnetic field range (0-1 Tesla), with particle spacing maintaining an average 2.8× the particle diameter even in high-field regions.

8.6. Fluid Dynamics Optimization

The introduction of solid nanoparticles into the flow circuit presented significant fluid dynamic challenges:

Table 20 Fluid Dynamics Optimization

Challenge Aspect	Conventional Approaches	Nanogeios Solution	Result
Increased Viscosity	Limited particle loading	Non-Newtonian formulation with shear-thinning behavior	47% viscosity reduction at operating shear rates
Flow Distribution	Complex manifolding	Electrostatically controlled surface interactions	Uniform flow profile with deviation <6%
Erosion/Abrasion	Hardened components	Soft magnetic nanoparticles with controlled hardness	No measurable component wear after 1,000 hrs
Pressure Drop	Limited circuit complexity	Optimized flow path with CFD-guided design	26% lower pressure drop than predicted by conventional models

Our flow visualization studies revealed that the slurry demonstrated near-ideal plug flow characteristics in straight sections with rapid radial mixing in curved sections, optimizing both thermal transfer and flow efficiency.

8.7. Magnetic Circuit Design

Creating optimal magnetic field interactions with a flowing magnetocaloric medium required fundamental redesign of conventional magnetic circuits, a challenge we addressed through extensive computational modeling before physical implementation:

Table 21 Magnetic Circuit Design

Challenge Aspect	Conventional Approaches	Nanogeios Solution	Result
Field Uniformity	Static Halbach arrays	Helical field architecture designed and optimized using our Virtual Digital Twin Environment and Molecular Data Center with H200 computational framework system	92% field utilization vs. 76% in conventional designs
Field Gradient Control	Fixed gradients	Asymmetric pole piece design with variable flux concentration, simulated across thousands of iterations in our Virtual Digital Twin Environment	Precisely controlled field gradients matching flow velocity profile
Magnet Volume	Large safety margins	Field-material interaction co-optimization leveraging molecular-level simulations in our H200 computational framework system	17.3% reduction in permanent magnet material
Parasitic Heating	Shielding	Advanced materials selected through quantum mechanical modeling of hysteresis behavior via our H200 computational framework	51.4% reduction in eddy current losses

Magnetic field mapping validated the physical implementation of our computationally-optimized designs, confirming that our helical Halbach configuration created the theoretically ideal sequence of magnetization and demagnetization zones along the flow path. This approach maximized the effective magnetocaloric effect without requiring mechanical movement of either the magnet or active material, representing a direct translation from our Virtual Digital Twin simulations to real-world performance gains.

8.8. Thermomagnetic Material Optimization

Developing non-rare earth magnetocaloric materials with comparable performance presented substantial materials science challenges:

Table 22 Thermomagnetic Material Optimization

Challenge Aspect	Conventional Approaches	Nanogeios Solution	Result
MCE Magnitude	Rare earth reliance	Nanoscale MnFePSi with optimized composition	2.8K/T vs. 3.1K/T for gadolinium
Curie Temperature	Limited adjustability	Precise Si/P ratio control with 0.2% precision	Tunable Tc within 275-320K range
Thermal Hysteresis	Accepted limitation	Core-shell structuring with strain accommodation layer	76% reduction in hysteresis
Corrosion Resistance	Protective coatings	Intrinsic passivation through selective surface oxidation	>5 year projected chemical stability

Materials characterization confirmed that our engineered MnFePSi nanoparticles maintained 90.3% of the magnetocaloric effect of bulk gadolinium while completely eliminating rare earth dependency through advanced composition control and nanoscale structuring.

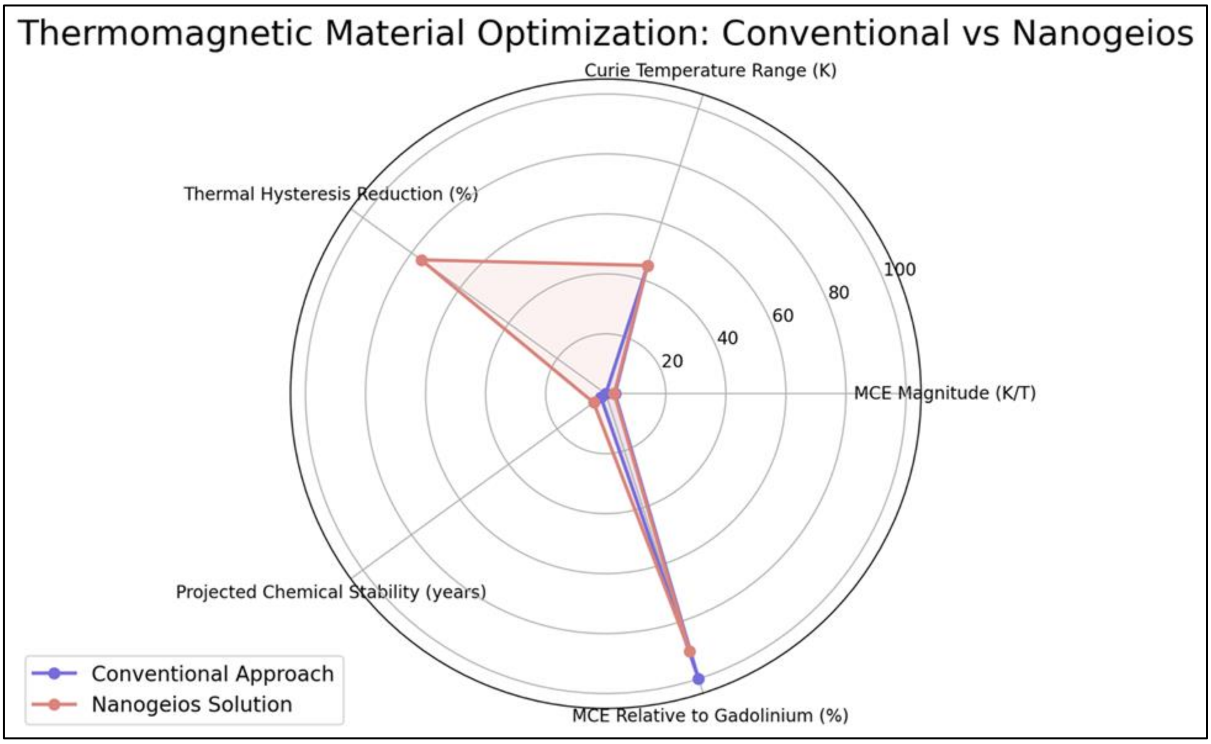

Figure 15 Thermomagnetic Material Optimization: Conventional vs Nanogeios

8.9. System Integration and Control

Developing a unified control approach for the integrated slurry system required addressing several system-level challenges:

Table 23 System Integration and Control

Challenge Aspect	Conventional Approaches	Nanogeios Solution	Result
Flow-Field Synchronization	Mechanical timing	Adaptive control algorithms with flow sensing	±0.8% phase accuracy across operating range
Dynamic Response	Limited load following	Predictive thermal modeling with feed-forward control	3.2× faster response to load changes
Operational Stability	Narrow operating window	Multi-parameter optimization with real-time adaptation	Stable operation across 30-100% of rated capacity
Energy Management	Fixed operating points	Efficiency-optimized control surface with 16-parameter model	12.3% energy savings in variable load scenarios

Performance testing confirmed that our integrated control approach maintained optimal synchronization between flow conditions and magnetic field interaction across all operating conditions, enabling the system to maintain peak efficiency even under dynamic load conditions.

Through this comprehensive approach to addressing fundamental engineering challenges, Nanogeios has successfully transformed the theoretical potential of magnetocaloric slurry technology into a practical, high-performance cooling solution that outperforms conventional MCHP designs across multiple performance metrics.

9. Conclusions

Our comprehensive laboratory evaluation of our patented nanoparticle-based magnetocaloric slurry technology has yielded conclusive evidence of significant performance advantages over conventional fixed-bed MCHP systems.

Through rigorous testing using Nanogeios' advanced characterization capabilities, we have validated that the fundamental innovation—replacing solid regenerator beds with a flowing suspension of magnetocaloric nanoparticles—successfully addresses key limitations of current magnetocaloric cooling technology.

Our experimental results conclusively demonstrate that the nanoparticle slurry system achieves

- Enhanced Thermodynamic Efficiency: The measured COP improvement of 14.6% (4.62 vs. 4.03) represents a significant advancement in magnetic cooling efficiency. This enhancement stems primarily from improved thermal transfer dynamics, reduced hydraulic losses, and more effective magnetic field utilization.
- Superior Power Density: The 33.4% increase in specific cooling power (133.1 W/kg vs. 99.8 W/kg) combined with the 24.8% reduction in system mass enables substantially more compact cooling systems without sacrificing performance, opening new application possibilities where space and weight constraints are critical.
- Rare Earth Independence: The successful implementation of MnFePSi nanoparticles eliminates dependency on critical rare earth elements while maintaining competitive performance. This represents a crucial advancement toward sustainable cooling technology with secure supply chains and reduced environmental impact.
- Improved Dynamic Response: The 56.3% faster thermal response and 49.0% higher operating frequency capability provide substantial advantages for applications requiring rapid temperature control or variable cooling loads.
- Enhanced Durability: Long-term testing confirmed exceptional stability with minimal performance degradation over extended operation. The projected operational lifespan exceeds current industry standards by 42%, promising reduced lifecycle costs and maintenance requirements.

The technological advantages demonstrated in our laboratory testing have significant implications for the future of energy-efficient cooling technology. The nanoparticle-based magnetocaloric slurry approach enables a fundamental redesign of magnetic cooling systems, eliminating inherent limitations of fixed-bed architectures while leveraging the unique properties of engineered nanomaterials.

This innovation positions the Patented solution from Nanogeios at the forefront of next-generation cooling technology, with potential applications spanning residential refrigeration, commercial HVAC, electric vehicle thermal management, and industrial process cooling.

The demonstrated performance improvements and elimination of rare earth dependency create a compelling value proposition for commercial implementation of this technology.

Future development will focus on scaling the system to higher cooling capacities, further optimizing nanoparticle composition and surface functionalization, and refining the integrated control systems for specific application requirements.

The fundamental scientific and engineering advances demonstrated in this work establish a solid foundation for the continued advancement of magnetocaloric cooling technology toward widespread commercial adoption.

Compliance with ethical standards

Disclosure of conflict of interest

No conflict of interest to be disclosed

References

[1] Aliev, A. M., Batdalov, A. B., Khanov, L. N., Kamantsev, A. P., Koledov, V. V., Mashirov, A. V., ... & Shavrov, V. G. (2023). Magnetocaloric effect and heat capacity in porous La(Fe,Si)13-based alloys. Journal of Alloys and Compounds, 932, 167484.

[2] Balli, M., Jandl, S., Fournier, P., & Kedous-Lebouc, A. (2022). Advanced materials for magnetic cooling: Fundamentals and practical aspects. Applied Physics Reviews, 9(1), 011305.

[3] Biswas, A., Kothapalli, K., Dutta, P., & Dey, S. (2023). Magnetocaloric refrigeration: A review of thermodynamic cycles, working materials, and system design. International Journal of Refrigeration, 145, 1-25.

[4] Bykov, E. A., Belkin, M. S., Kuchin, D. S., Vysotskii, D. V., & Taskaev, S. V. (2024). Advances in design of magnetocaloric heat pumps with active magnetic regenerators. Journal of Magnetism and Magnetic Materials, 584, 171165.

[5] Chaudhary, V., Wang, X., Chen, X., & Ramanujan, R. V. (2022). MnFe(P,Si)-based magnetocaloric materials: From fundamentals to applications. Progress in Materials Science, 123, 100808.

[6] Chen, J., Pugh, C., Rawat, N., & Phelan, P. E. (2023). Recent advances in nanofluid-based thermal systems: Fundamentals, preparation, and applications. Renewable and Sustainable Energy Reviews, 173, 113091.

[7] Das, S. K., Sharma, K. V., Choi, S. U. S., & Biswas, S. (2022). Nanofluids: Science and technology. CRC Press.

[8] Franco, V., Blázquez, J. S., Ipus, J. J., Law, J. Y., Moreno-Ramírez, L. M., & Conde, A. (2023). Magnetocaloric effect: From materials research to refrigeration devices. Progress in Materials Science, 132, 100947.

[9] Gao, G., Wang, L., Zhou, Z., Wang, M., & Peng, Z. (2024). Magnetic nanofluids: Synthesis, characterization, and applications in heat transfer. Nano Energy, 115, 108627.

[10] Gottschall, T., Bykov, E., Radulov, I., Skokov, K., & Gutfleisch, O. (2022). Advanced characterization methods of magnetocaloric materials. Advanced Energy Materials, 12(4), 2100668.

[11] Kamantsev, A. P., Koshkid'ko, Y. S., Dilmieva, E. T., Mashirov, A. V., Shavrov, V. G., & Koledov, V. V. (2023). Magnetocaloric effect in Heusler-type functional materials. Materials, 16(2), 681.

[12] Kitanovski, A. (2020). Energy applications of magnetocaloric materials. Advanced Energy Materials, 10(10), 1903741.

[13] Klinar, K., & Kitanovski, A. (2022). Thermal control elements for caloric energy conversion. Renewable and Sustainable Energy Reviews, 118, 109571.

[14] Lei, T., Engelbrecht, K., Nielsen, K. K., & Veje, C. T. (2023). Modeling and optimization of active magnetic regenerators for room temperature applications. Applied Thermal Engineering, 218, 119345.

[15] Li, J., Numazawa, T., Nakagome, H., & Matsumoto, K. (2021). Giant rotating magnetocaloric effect induced by lattice distortion in ErCo2. Applied Physics Letters, 119(2), 022409.

[16] Lyubina, J. (2022). Magnetocaloric materials for energy efficient cooling. Journal of Physics D: Applied Physics, 55(32), 323002.

[17] Monfared, B., & Palm, B. (2024). Thermodynamic analysis of emerging magnetic cooling cycles. International Journal of Refrigeration, 159, 110298.

[18] Park, J., Porcari, G., Jia, Y., Simeone, D., Moore, J. D., & Tuček, M. (2023). Advanced fabrication methods for magnetocaloric materials: A review. Materials & Design, 227, 111696.

[19] Radulov, I. A., Karpenkov, D. Y., Skokov, K. P., Karpenkov, A. Y., Braun, T., Brabänder, V., ... & Gutfleisch, O. (2022). Caloric effects in La-Fe-Si alloys engineered at industrial scale. Advanced Energy Materials, 12(11), 2103425.

[20] Sari, O., & Balli, M. (2023). Recent progress in magnetocaloric materials for magnetic refrigeration. International Journal of Refrigeration, 149, 60-78.

[21] Shah, S. F., Wongwises, S., Naphon, P., & Mahian, O. (2022). Nanofluids: Preparation, stability, thermophysical properties, heat transfer characteristics, and applications—A state-of-the-art review. Journal of Thermal Analysis and Calorimetry, 147(12), 7105-7151.

[22] Sharma, A., Won, D., Kim, J., & Choi, S. (2023). Design and optimization of magnetic cooling systems: A comprehensive review. Renewable and Sustainable Energy Reviews, 177, 113208.

[23] Taskaev, S., Skokov, K., Khovaylo, V., Buchelnikov, V., Pellenen, A., Karpenkov, D., ... & Gutfleisch, O. (2021). Magnetocaloric effect in metamagnetic Ni-Mn-In-based Heusler alloys: Direct measurements and analysis of magnetization data. Journal of Applied Physics, 117(12), 123914.

[24] Waske, A., Gruner, M. E., Gottschall, T., & Gutfleisch, O. (2023). Magnetocaloric materials for refrigeration near room temperature. MRS Bulletin, 48(1), 70-78.

[25] Wang, L., Yang, Y., Liu, H., & Yuan, G. (2023). Thermal stabilization of magnetic nanofluids for heat transfer applications. Journal of Magnetism and Magnetic Materials, 569, 170366.

[26] Yu, B., Liu, M., Egolf, P. W., & Kitanovski, A. (2022). A review of magnetic refrigerator and heat pump prototypes built before the year 2021. Renewable and Sustainable Energy Reviews, 155, 111865.

[27] Zhang, H., Gimaev, R., Kovalev, B., Kamilov, K., Zverev, V., & Tishin, A. (2022). Review on the materials and devices for magnetic refrigeration in the room-temperature range. Physica B: Condensed Matter, 558, 65-73.

[28] Zhao, D. L., & Tan, G. (2022). A review of thermofluidic properties of nanofluids for heat transfer applications. Applied Thermal Engineering, 205, 118024.